# Detection of early signs of right ventricular systolic impairment in unoperated Ebstein's anomaly by cardiac magnetic resonance feature tracking

**Francesca Baessato[1,2], Claudia Furtmüller[1], Nerejda Shehu[1], Irene Ferrari[1], Bettina Reich[1], Nicole Nagdyman[1], Stefan Martinoff[3], Heiko Stern[1], Peter Ewert[1], Christian Meierhofer[1]**

[1]Congenital Heart disease and Pediatric Cardiology, German Heart Center Munich, Technical University of Munich, Munich, Germany; [2]Department of Cardiology, Regional Hospital S. Maurizio, Bolzano, Italy; [3]Department of Radiology, German Heart Center Munich, Technical University of Munich, Munich, Germany

*Contributions:* (I) Conception and design: F Baessato, C Meierhofer; (II) Administrative support: C Meierhofer; (III) Provision of study materials or patients: All authors; (IV) Collection and assembly of data: F Baessato, C Furtmüller, C Meierhofer; (V) Data analysis and interpretation: F Baessato, C Furtmüller, C Meierhofer; (VI) Manuscript writing: All authors; (VII) Final approval of manuscript: All authors.

*Correspondence to:* Dr. Francesca Baessato. Department of Cardiology, Regional Hospital S. Maurizio, Via Lorenz Böhler 5, 39100 Bolzano, Italy. Email: francesca.baessato89@gmail.com.

**Background:** Cardiovascular magnetic resonance feature-tracking analysis (CMR-FT) provides a quantitative assessment of myocardial contraction with potential for diagnostic and prognostic ability in a wide spectrum of diseases. Ebstein's anomaly (EA) is a rare congenital heart disease characterized by apical displacement of the tricuspid valve. However, it is also considered a disorder of development affecting the global right ventricular myocardium. Aim of our study is to describe the complex contractile mechanics of the functional right ventricle (RV) in patients affected by EA through CMR-FT.

**Methods:** Fifty surgery-free EA patients who had undergone a complete CMR protocol at our institution between January 2017 and December 2020 were selected for the retrospective study. A historical control group of twenty-five healthy subjects was also included. CMR-FT analysis was performed at a dedicated workstation by manually tracing RV endo- end epicardial borders on steady-state-free-precession (SSFP) cine images. Strain values were calculated. Apical displacement of the tricuspid valve (TV) was measured on a 4-chamber cine image from the right atrio-ventricular junction to the functional annulus of the TV.

**Results:** EA patients presented significantly impaired RV global radial strain (GRS) and global circumferential strain (GCS) compared to controls (P<0.0001 and P=0.0008, respectively). In a subgroup analysis, GRS was significantly compromised in patients with a severely displaced TV (>16 mm/m$^2$) compared to milder forms (P=0.03) and to controls (P<0.0001). Among EA patients with a preserved ejection fraction, 12 (48%) *vs.* 6 (24%) controls had reduced both GRS and GCS.

**Conclusions:** The contractile pattern of the functional RV in EA is characterised by prevalent alterations in the short-axis direction as indicated by reduced GRS and GCS. Strain values might be reduced prior to routine used functional parameters like RV ejection fraction (RVEF) and can possibly serve as an early predictor of myocardial dysfunction in EA patients.

**Keywords:** Congenital heart disease; cardiovascular magnetic resonance; feature tracking; myocardial deformation

## Introduction

Cardiac magnetic resonance (CMR) is considered the gold standard for the assessment of the volumes and function of the right ventricle (RV), with growing importance in both diagnostic follow-up and pre-procedural planning of congenital heart diseases (1,2). CMR feature-tracking (CMR-FT) allows a quantitative and non-invasive evaluation of both global and segmental function of the cardiac muscle. Strain values are given by the entity of myocardial displacement in systole calculated through a frame-to-frame automatic tracking of an initial contouring along the cardiac cycle (3). Relevant advantages of CMR-FT compared to other strain modalities, such as CMR tissue tagging, are that it involves only commonly acquired cine images without any need for additional sequences, and has significantly reduced post-processing times (4). CMR-FT of the left ventricle (LV) has already shown a powerful diagnostic and prognostic ability as demonstrated in studies concerning dilated cardiomyopathy, cardiac amyloidosis, and heart failure with preserved ejection fraction (5,6). CMR-FT may allow a detailed contouring of the RV despite its thin myocardial wall and diffuse trabeculations (7). This tool may potentially elucidate subtle alterations in the mechanics of the myocardium that are not achieved by routine cardiac imaging techniques. Recently, RV myocardial strain has been found to be impaired in many cardiac diseases. These include congenital heart defects, pulmonary hypertension, and cardiac insufficiency (8).

Ebstein's anomaly (EA) represents less than 1% of all congenital cardiac defects and is characterized by apical displacement of the functional annulus of the tricuspid valve (TV) (9,10). The septal and posterior leaflets of the TV fail to delaminate from the primitive myocardium during the embryologic development, resulting in atrialization of a portion of the RV with dilatation and volume overload due to tricuspid regurgitation (11). Although it is principally seen as a disease of the TV, EA is characterized by global alterations of the RV myocardium (12,13).

Different CMR parameters including RV ejection fraction (RVEF) have been proposed to monitor the progression of disease (14). The aim of our study was to characterize the abnormal mechanics of the functional RV in unoperated EA patients through CMR-FT analysis. Moreover, we aimed to assess whether initial RV systolic dysfunction could be reliably evidenced by CMR-FT also in cases where routine CMR gives a still preserved RVEF. We present the following article in accordance with the STROBE reporting checklist (available at https://cdt.amegroups.com/article/view/10.21037/cdt-22-82/rc).

## Methods

### *Study population*

Unoperated patients with EA who underwent a CMR examination at our centre from January 2017 to December 2020 were identified retrospectively. Seventeen patients aged <18 years were also included in the population study, neonates or infants were excluded. A study flowchart is depicted in *Figure 1*. All patients underwent a complete standardized CMR protocol in the context of their routine clinical controls. Medical history, clinical assessment, electrocardiogram (ECG) features (QRS duration) and New York Heart Association (NHYA) functional class were also assessed for each patient. Additionally, a historical control group of twenty-five healthy subjects with no evidence of cardiac disease at the timepoint of the study was included. Baseline characteristics of EA patients and controls are shown in *Tables 1,2*. The study was conducted in accordance with the Declaration of Helsinki (as revised in 2013). The study was approved by the ethical review board of the Technical University of Munich (No. 213/21 S-KK) and individual consent for this retrospective analysis was waived.

### *CMR acquisition protocol*

All patients were studied with a 1.5 Tesla MRI scanner (MAGNETOM Avanto®, Siemens Healthineers, Erlangen, Germany) using a 12-element cardiac phased array coil. For volumetric assessment, axial, multiphase, breath-hold, steady-state-free-precession (SSFP) cine sequences with retrospective ECG-gating were performed. Breath-holding was achieved during expiration. A stack of axial slices was obtained from the coronal and sagittal localizers in order to cover the heart from just below the diaphragm to the pulmonary bifurcation (slice thickness of 4 to 8 mm according to body weight, 25 phases/cardiac cycle, 1 slice per 8–12 s breath-hold, an acquisition matrix of 192×192) (15). Displacement of the TV leaflets was assessed in a 4-chamber SSFP cine image by measuring the distance from the septal leaflet to the right atrio-ventricular junction, indexed to the body surface area (BSA) (16). Flow measurements were obtained using two-dimensional (2D) phase contrast images. For most patients, the regurgitant volume and the regurgitant fraction of the
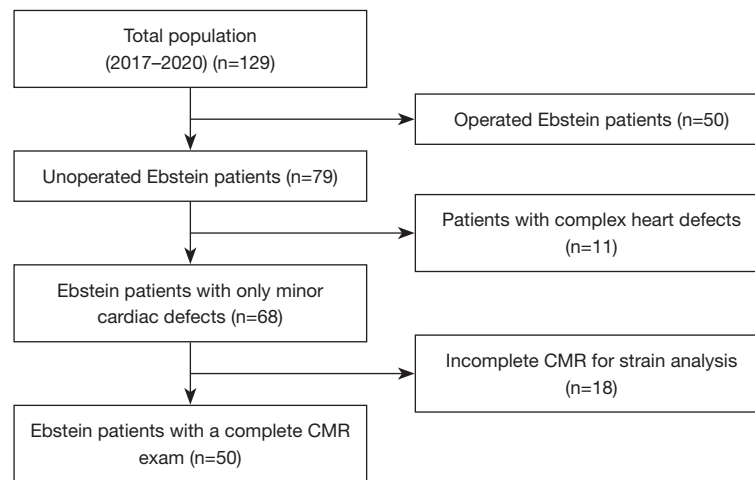
```
Total population
(2017–2020) (n=129)
         │
         │──────────────────►  Operated Ebstein patients (n=50)
         ▼
Unoperated Ebstein patients (n=79)
         │
         │──────────────────►  Patients with complex heart defects
         ▼                      (n=11)
Ebstein patients with only minor
cardiac defects (n=68)
         │
         │──────────────────►  Incomplete CMR for strain analysis
         ▼                      (n=18)
Ebstein patients with a complete CMR
exam (n=50)
```

**Figure 1** Flowchart of the study with initial screening and selection of unoperated patients with Ebstein's anomaly who underwent a complete CMR examination in the context of their clinical routine controls. CMR, cardiovascular magnetic resonance.

**Table 1** Baseline characteristics of patients with Ebstein's anomaly and controls

| Clinical parameters | Ebstein's patients (n=50) | Controls (n=25) | P value |
|---|---|---|---|
| Age at CMR examination (years) | 31.5±19.3 | 22.4±8.1 | 0.0271 |
| Height (m) | 1.6±0.2 | 1.8±0.1 | 0.0016 |
| Weight (kg) | 61.90±20.7 | 68.20±12.48 | 0.2713 |
| Body surface area (kg/m$^2$) | 64.0±32.4 | 34.9±8.2 | 0.1127 |
| BMI (kg/m$^2$) | 22.2±4.2 | 21.7±3.1 | 0.3603 |
| Heart rate (min$^{-1}$) | 75.3±16.4 | 68.56±8.9 | 0.0586 |
| QRS duration (ms) | 120.7±29.7 | | |
| Systolic blood pressure (mmHg) | 116.4±20.1 | | |
| Diastolic blood pressure (mmHg) | 73±11.4 | | |

CMR, cardiovascular magnetic resonance; BMI, body mass index.

TV were assessed using en-face phase contrast images of the displaced TV orifice. When technically not feasible, only the indirect measure obtained from the volumetric assessment and the forward flow through the pulmonary valve was given. Comprehensively, there was no significant difference between direct (en-face) and indirect measure of tricuspid regurgitation (35.95±19.45 *vs.* 35.89±17.66, P=0.98). All CMR data were transferred to a dedicated workstation (Circle Cardiovascular Imaging Inc., CVI42® 5.12.1 software, Calgary, Alberta) for post-processing. For volumetric assessment, endocardial contours of the functional RV and of the LV were manually traced in the axial slices in both end-systole and end-diastole, excluding papillary muscles and trabeculations, which were considered part of the cardiac mass. Volumetric measures were reported indexed to BSA. Previous works have proved high reproducibility and accuracy of CMR volume analysis in patients with congenital heart diseases and EA at our centre (17,18).

### CMR-FT

CMR-FT analysis was performed using Circle CVI42 5.12.1 software (Tissue Tracking, Circle Cardiovascular Imaging Inc., CVI42® 5.12.1 software, Calgary, Alberta). Endocardial and epicardial contours of the functional RV were manually traced in long-axis and short-axis SSFP cine images at end-

**Table 2** Medications and clinical characteristics of Ebstein's anomaly patients

| Parameters | n (%) |
|---|---|
| Male/female | 28 (56.0)/22 (44.0) |
| Medication | |
| ACE inhibitors/sartans | 3 (6.82) |
| Beta-blockers | 6 (13.64) |
| Diuretics | 5 (11.36) |
| Antiarrhythmics | 1 (2.27) |
| ASA/anticoagulants | 10 (22.73) |
| NYHA class | |
| NYHA 1 | 30 (61.22) |
| NYHA 2 | 14 (28.57) |
| NYHA 3 | 5 (10.20) |
| NYHA 4 | 0 (0.0) |
| Additional congenital heart defects | 23 (47.92) |
| ASD | 18 (37.5) |
| VSD | 1 (2.08) |
| Valve disease | 4 (8.33) |
| Arrhythmias | 16 (39.02) |
| Heart failure progression | 3 (7.32) |
| Need for surgery | 18 (43.90) |

ASA, acetylsalicylic acid; NHYA, New York Heart Association; ASD, atrial septal defect; VSD, ventricular septal defect.

diastole. All contours were then automatically propagated through the cardiac cycle by applying the dedicated algorithm. If the automatic tracking was considered visually inadequate, SSFP cine images were retracked and the algorithm reapplied. Global peak systolic radial strain (GRS) and global peak systolic circumferential strain (GCS) were derived from short-axis images (basal, mid-ventricular, apical slices) while a 4-chamber cine image was used to quantify global peak systolic longitudinal strain (GLS). To determine the reproducibility of our measurements, CMR-FT analysis was evaluated twice by two blinded expert readers in a group of 10 randomly selected patients.

*Statistical analysis*

Continuous variables are reported as mean ± SD or median with ranges. Categorical data are plotted as frequencies

(percentages). Normal distribution of all variables was assessed with the Kolmogorov-Smirnov test. Continuous comparisons of two groups were performed with the unpaired two-tailed Student's *t*-test or Mann-Whitney test, while for continuous comparisons of three groups, one-way ANOVA or Kruskall Wallis test were used. Preserved RVEF was defined when >52%. Best cut-off values for CMR-FT were identified using receiver operating characteristic (ROC) curves by assessing the values with highest sensitivity and specificity. Intraobserver and interobserver variabilities of CMR-FT were assessed with the Bland-Altman analysis in terms of mean difference and limits of agreement. Results were considered significant with P values <0.05 (two-tailed). Statistical analysis was performed using the software GraphPad Prism (GraphPad Prism® version 9.2.0, GraphPad Software Inc., La Jolla, CA).

## Results

A total of 50 patients with unoperated EA were included. Age was 2 to 72 years (median 29 years). Twenty-eight patients were males (56%), 22 were females (44%). The majority were in NHYA class I (30, 61.22%) or class II (14, 28.57%), only five patients were in class III (10.2%) and none was in class IV (0%). Twenty-three patients (47.92%) had other minor congenital anomalies, predominantly small atrial septal defects, but with no evidence of hemodynamically relevant shunt, as all Qp/Qs ratio values were between 0.9 and 1.2. Among control subjects, 20 subjects were males (80%), 5 were females (20%). Mean age was 22.40±8.057 years. *Table 3* shows a comparison of CMR data between EA patients and controls. RV global systolic function expressed by RVEF was significantly lower in EA than in controls (51.8%±9.2% *vs.* 60.6%±4.3%, P<0.0001). Both indexed RV end-diastolic (RVEDVI) and end-systolic (RVESVI) volumes were higher in EA than in controls (130.2±54.4 *vs.* 88.6±17.9, P<0.0001 and 64.0±32.4 *vs.* 34.9±8.2, P<0.0001, respectively). Left ventricular ejection fraction (LVEF) was also significantly reduced (60.2±7.3 *vs.* 67.4±6.6, P<0.0001), but with smaller end-diastolic volumes (60.4±11.8 *vs.* 83.2±17.4, P<0.0001) in EA patients than in controls.

CMR-FT was performed on the RV in all patients. In two cases GRS and GCS values were excluded due to technical reasons. Comprehensively, GRS and GCS were significantly compromised in EA compared to control subjects (19.2±7.6 *vs.* 29.2±9.5, P<0.0001 and −12.2±4.5

**Table 3** Cardiovascular magnetic resonance characteristics of Ebstein's anomaly compared to controls

| CMR parameters | Ebstein's patients (n=50) | Controls (n=25) | P value |
|---|---|---|---|
| RVEF (%) | 51.8±9.2 | 60.6±4.3 | <0.0001 |
| RVEDVi (mL/m$^2$) | 130.2±54.4 | 88.6±17.9 | 0.0001 |
| RVESVi (mL/m$^2$) | 64.0±32.4 | 34.9±8.2 | <0.0001 |
| RVSVi (mL/m$^2$) | 66.3±27.5 | 53.9±11.5 | 0.0517 |
| LVEF (%) | 60.2±7.3 | 67.4±6.6 | <0.0001 |
| LVEDVi (mL/m$^2$) | 60.4±11.8 | 83.2±17.4 | <0.0001 |
| LVESVi (mL/m$^2$) | 24.2±7.5 | 27.1±7.6 | 0.1073 |
| LVSVi (mL/m$^2$) | 36.2±7.2 | 56.1±13.1 | <0.0001 |
| Global radial strain (%) | 19.2±7.6 | 29.18±9.49 | <0.0001 |
| Global circumferential strain (%) | −12.2±4.5 | −15.88±3.91 | 0.0008 |
| Global longitudinal strain (%) | −18.4±4.0 | −19.6±3.7 | 0.2121 |
| TI direct (%) | 35.95±19.45 | | |
| TI indirect (%) | 35.89±17.66 | | |
| TV displacement indexed (mm/m$^2$) | 18.02±7.771 | | |
| PA flow net indexed (mL/m$^2$) | 37.47±8.337 | | |
| PA flow antegrade indexed (mL/m$^2$) | 38.45±8.307 | | |
| Cardiac index PA (L/min/m$^2$) | 2.80±0.791 | | |
| Aorta flow net indexed (mL/m$^2$) | 37.58±7.562 | | |
| Aorta flow antegrade indexed (mL/m$^2$) | 38.16±7.622 | | |
| Cardiac index aorta (L/min/m$^2$) | 2.80±0.7808 | | |

CMR, cardiovascular magnetic resonance; RV, right ventricle; EF, ejection fraction; EDVi, indexed end-diastolic volume; ESVi, indexed end-systolic volume; SVi, indexed stroke volume; LV, left ventricle; TI, tricuspid insufficiency; TV, tricuspid valve; PA, pulmonary artery.

*vs.* −15.9±3.9, P=0.0008, respectively), while no statistical difference was noted for GLS (−18.4±4.0 *vs.* −19.6±3.7, P=0.2121), as illustrated in *Figure 2*. *Figure 3* shows a representative case.

In a subgroup analysis, comparisons were made between forms of EA with severe displacement of the TV (indexed TV apical displacement >16 mm/m$^2$) and less severe forms (indexed apical displacement ≤16 mm/m$^2$), as well as with controls. GRS was significantly reduced in most advanced EA forms compared to patients with less displaced TV (16.9±8.3 *vs.* 21.5±6.2, P=0.0348) and to controls (29.2±9.5, P value among the three groups <0.0001) (*Figure 4*). RV volumes were also significantly increased in more severe cases (RV end-diastolic volume indexed 145.5±64.4 *vs.* 114.9±37.4, P=0.0457) with reduced LV systolic function (LV EF 57.8±7.0 *vs.* 62.6±7.0, P=0.0215), as shown in *Table 4*.

Twenty-five EA patients had an RVEF >52%. To evaluate if strain analysis could identify initial alterations of myocardial deformation and systolic dysfunction of the RV, ROC curves were used to find the best thresholds of CMR-FT radial [area under the curve (AUC) 0.77, P=0.0001] and circumferential (AUC 0.74, P=0.001) strain values to discriminate EA from controls. Cut-off values for GRS and GCS were 23.68% (sensitivity, 69%; specificity, 68%) and −13.95% (sensitivity, 67%; specificity, 72%), respectively. Based on these cut-offs, a scatterplot was developed with the GRS and GCS values among EA patients with RVEF >52% and controls (*Figure 5*). Twelve (48%) EA patients with still preserved RVEF *vs.* six (24%) controls presented a GRS <23.68% and a GCS >−13.95%. In opposition, sixteen (64%) controls *vs.* eight (32%) EA patients had a GRS >23.68% and a GCS <−13.95%.
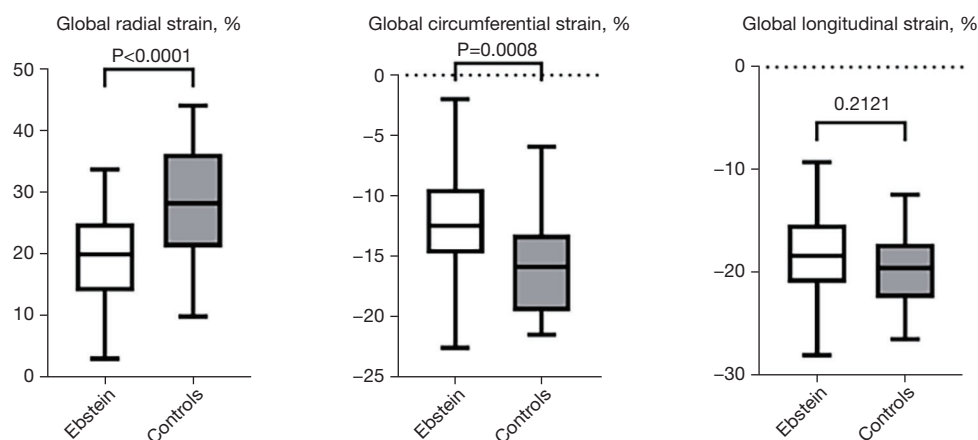
**Figure 2** Comparison of strain values between patients with Ebstein's anomaly and healthy subjects represented by Tukey's boxplots. Both global radial and circumferential strain are significantly reduced compared to controls (P<0.0001 and P=0.0008, respectively), while no significant difference was evidenced for GLS (P=0.2121). GLS, global longitudinal strain.
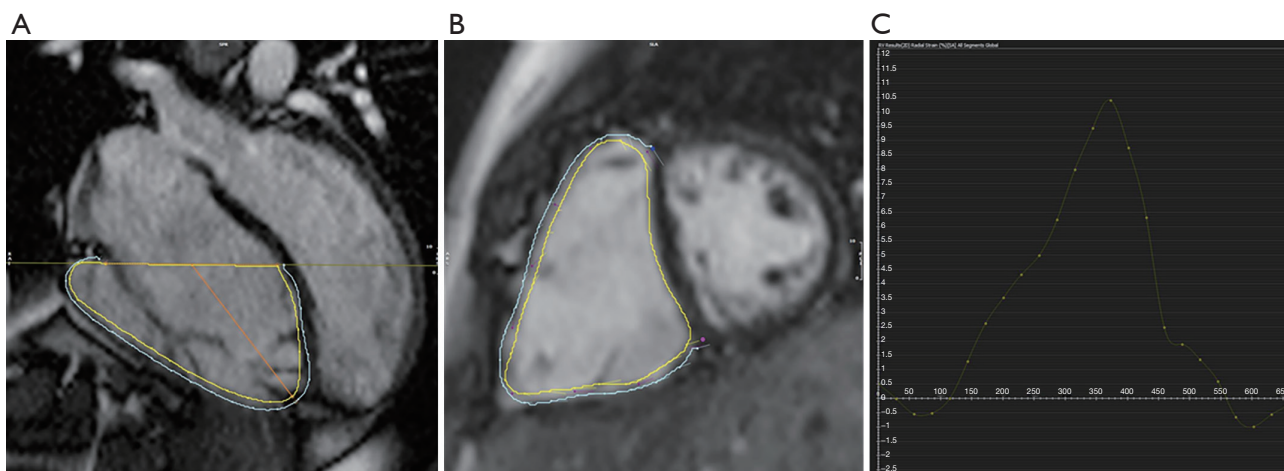


**Figure 3** Male, 29 years old, affected by Ebstein anomaly. The functional right ventricle is dilated (end-diastolic volume 111 mL/m$^2$) with moderate systolic dysfunction (ejection fraction 44%). Strain values are derived from accurate contouring of endocardial and epicardial borders in the 4-chamber cine and in the short-axis images, as shown in panel A and B. In this patient, peak systolic global radial strain is only 10.5% (C).

The results of the Bland-Altman analysis showed adequate reproducibility of repeated data with limited bias and narrow limits of agreement (LOA) for all GRS (intraobserver: bias, –0.5%; lower LOA, –6.2%; upper LOA, 5.1%; interobserver: bias, –0.99%; lower LOA, –7.7%; upper LOA, 5.8%), GCS (intraobserver: bias, 0.6%; lower LOA, –1.9%; upper LOA, 3.0%; interobserver: bias, 0.9%; lower LOA, –2.0%; upper LOA, 3.9%), and for GLS (intraobserver: bias, –1.8%; lower LOA, –6.3%; upper LOA, 2.8%; interobserver: bias, –0.5%; lower LOA, –3.7%; upper LOA, 2.7%).

## Discussion

The main findings of this study are that in patients with EA, the functional RV is characterized by (I) significantly lower GRS and GCS than in healthy subjects; (II) higher contractile dysfunction along the short-axis direction in
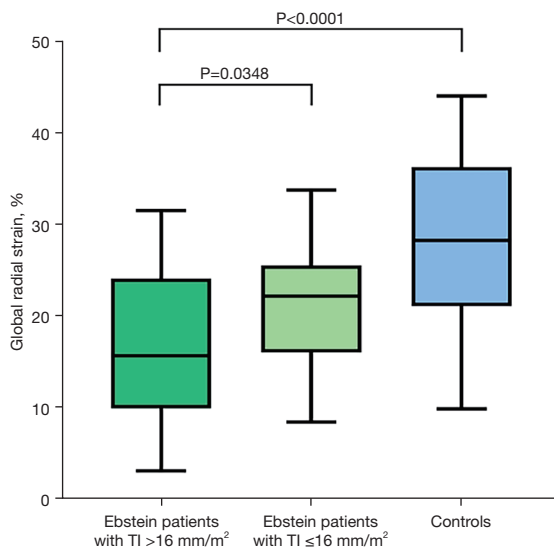
284

**Baessato et al. Feature tracking analysis in unoperated Ebstein's anomaly**



**Figure 4** A progressive deterioration in radial deformation is observed in Ebstein's anomaly patients with higher severity of apical displacement of the tricuspid valve leaflets. In most advanced disease (apical displacement >16 mm/m$^2$) global radial strain is significantly lower compared to the group with less severe disease (apical displacement ≤16 mm/m$^2$) (P=0.0348). A significant reduction of radial strain is observed also among the disease groups and healthy subjects (P<0.0001).

cases with more severe displacement of the TV; (III) good reproducibility of strain values; (IV) presence of subtle signs of cardiac deterioration detected through CMR-FT that are not commonly detected by routine CMR parameters. Although the diagnosis of EA is given by the presence of TV alterations, the disease also involves the myocardium which may contribute to alterations in ventricular geometry and systolic function (19). CMR-FT represents a reliable tool of advanced cardiac imaging which quantitively assesses cardiac contractility and may add prognostic information in EA as already observed in some congenital heart diseases (20). In our study we aimed to fully describe the contraction pattern of the functional RV in EA and evidenced a significant reduction of both GCS and GRS. In all our cases of EA, the functional RV was purely volume overloaded due to tricuspid regurgitation (median 35% regurgitation fraction). A previous study by Lee *et al.* in patients affected by EA first assessed the three-dimensional shape of the functional RV. The authors highlighted a predominant short-axis contraction impairment, with no reduction of longitudinal shortening (21), which is in line with our results. These alterations of strain values in EA could be justified not also by intrinsic myocardial impairment, but also by volume overload due

**Table 4** Subgroup analysis of Ebstein's anomaly patients with less and more severe disease defined by the displacement of the tricuspid valve and controls

| Parameters | EA with TV displacement >16 mm/m$^2$ (n=25) | EA with TV displacement ≤16 mm/m$^2$ (n=25) | P value (2 groups) | Controls (n=25) | P value (3 groups) |
|---|---|---|---|---|---|
| Global RS (%) | 16.91±8.297 | 21.51±6.207 | 0.0348 | 29.18±9.49 | <0.0001 |
| Global CS (%) | −11.08±4.986 | −13.17±3.742 | 0.106 | −15.88±3.91 | 0.0009 |
| Global LS (%) | −19.11±4.52 | −17.72±3.3 | 0.1744 | −19.61±3.68 | 0.1344 |
| RVEF (%) | 49.36±9.28 | 54.28±8.52 | 0.0569 | 60.60±4.3 | <0.0001 |
| RVEDVi (mL/m$^2$) | 145.50±64.4 | 114.90±37.44 | 0.0457 | 88.60±17.9 | 0.0001 |
| RVESVi (mL/m$^2$) | 73.48±34.69 | 54.44±27.48 | 0.0162 | 34.90±8.2 | <0.0001 |
| RVSVi (mL/m$^2$) | 72.04±35.77 | 60.56±13.85 | 0.1411 | 53.90±11.5 | 0.0236 |
| LVEF (%) | 57.84±7.05 | 62.56±6.98 | 0.0215 | 67.40±6.6 | <0.0001 |
| LVEDVi (mL/m$^2$) | 59.88±10.86 | 60.96±12.82 | 0.7493 | 83.20±17.4 | <0.0001 |
| LVESVi (mL/m$^2$) | 25.40±7.45 | 23.08±7.43 | 0.276 | 27.10±7.6 | 0.8747 |
| LVSVi (mL/m$^2$) | 34.48±6.31 | 37.84±7.69 | 0.0978 | 56.10±13.1 | <0.0001 |
| TI direct (%) | 32.30±17.18 | 40.15±21.44 | 0.1903 | – | – |

EA, Ebstein's anomaly; TV, tricuspid valve; RS, radial strain; CS, circumferential strain; LS, longitudinal strain; RV, right ventricle; EF, ejection fraction; EDVi, indexed end-diastolic volume; ESVi, indexed end-systolic volume; SVi, indexed stroke volume; LV, left ventricle; TI, tricuspid insufficiency.
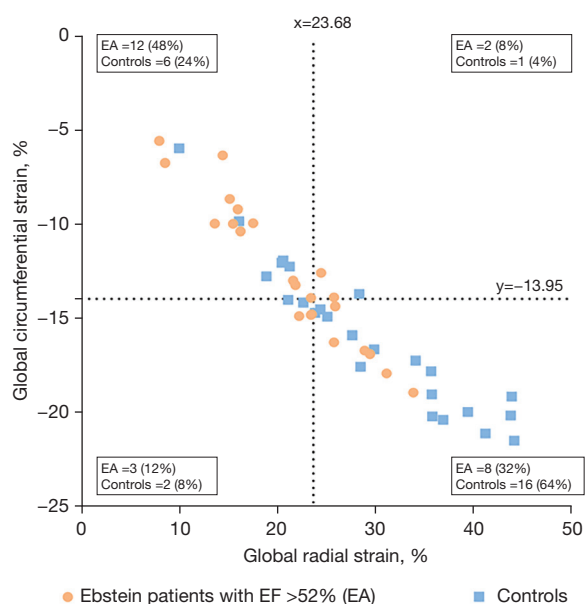
**Figure 5** Among all EA patients with preserved systolic function as expressed by an EF >52%, 12 (48%) already presented a reduction of both global radial and circumferential strain (based on cut-off values of 23.68% and –13.95%, respectively). Eight (32%) patients had normal strain values, while other three (12%) and two (8%) patients showed reduction of only radial strain and circumferential strain, respectively. EF, ejection fraction; EA, Ebstein's anomaly.

than circumferential free wall strain values. It was hypothesized that in pressure loaded RV, predominant circumferential over longitudinal shortening occurs as an adaptive mechanism to systemic pressure (25). These findings in pressure overloaded RV are the opposite to our results that occurred in pure volume overloaded RV, where the longitudinal component of contraction is preserved and circumferential displacement is compromised. Studies on volume-overloaded LV due to severe mitral regurgitation also showed a relevant impairment of GCS (26).

In the last few years, some research studies have focused on strain analysis in EA patients. In 2016, Kühn *et al.* demonstrated how among all echocardiographic parameters of RV function, 2D RV GLS best correlated with CMR-derived RVEF in patients with EA (27). Steinmetz *et al.* demonstrated in EA patients reduction of the reservoir and booster pump function of the RA with CMR-FT, which is related to heart failure markers such as NHYA class and brain natriuretic peptide (BNP) (28). Concerning the RV, neither GRS nor GCS was investigated. In our study we evaluated the short-axis component of RV contraction since it was hypothesized that in cases of abnormal loading conditions, such as EA, shortening of circumferential fibres may contribute differently to RV systolic function than in normal hearts (29). Recently, CMR-FT and four dimensional-volume analysis underlined how EA patients also presented high LV intraventricular dyssynchrony, which related to ECG alterations, higher functional NHYA class and more severe forms of disease (30).

Definition of EA is given by the entity of the anatomical displacement of the septal leaflet of the TV from the atrio-ventricular junction, and we evaluated the severity of disease based on the entity of displacement. This is a pure anatomical parameter and does not represent per se an indicator of clinical disease severity. However, it has already been demonstrated how the degree of functional TV annular displacement determines much of the clinical outcome in EA, and higher degrees of displacement have been related to a reduced functional capacity of the RV (10). In a subgroup of patients with severe apical displacement of the TV, we observed a significant reduction of GRS compared to other patients with less severe disease and to controls. In this subgroup of EA also GCS was, though not significantly, reduced. It would be questionable if the modifications in the contraction pattern in EA patients may effectively represent a sign of incipient myocardial dysfunction or are only an adaptive response to the change of the hemodynamic status. Structural alterations of the RV

to tricuspid regurgitation. However, comparison data with patients with functional tricuspid regurgitation are lacking and should be implemented by larger, randomized, prospective studies. Interestingly, the reduction of GCS and GRS as a consequence of myocardial alterations seems to be further supported by pathological studies. It was described how in EA the RV free wall is typically thinner and presents fewer circumferential fibres than in normal hearts (22). Moreover, a relevant enlargement of the RV atrio-ventricular junction was described (23). In opposition, histological studies on pressure overloaded RV described a prevalent hypertrophy of middle-layer circumferential fibres (24). In our study, GLS is not significantly impaired. This could be interpreted as an intrinsic myocardial compensatory mechanism to reduction of circumferential shortening. CMR studies performed in pressure loaded RV such as in systemic RV or tetralogy of Fallot demonstrated how in cases of RV hypertrophy GCS exceed GLS, with a shift from longitudinal to circumferential shortening. Differently, in normal RV there were higher longitudinal

in EA have been observed in recent CMR studies which confirmed the presence of diffuse and regional fibrosis in the RV myocardium, which is related to the degree of RV dilatation and a worse NYHA class (31). In our study although most patients presented with NHYA class I or II, there was a significant reduction of RVEF compared to controls.

We hypothesize that in EA there is a relevant impairment in terms of the transverse component of myocardial contraction, which may predominantly justify the reduction of RVEF. Among EA patients with a still preserved RV systolic function, we found that many already presented reduction of both GCS and GRS. Reduced strain values were observed also in six controls with normal RVEF; these patients were recruited as healthy subjects at the timepoint of the study.

Some authors underlined how the performance of radial and circumferential strain may be not feasible in the RV due to the thin wall thickness and severe trabeculations (32). With our study we demonstrated that CMR-FT is a suitable technique for quantitative determination of cardiac deterioration in complex congenital heart disease such as EA. Other studies also determined adequate reproducibility of circumferential and radial strain values on the RV, underlying how CMR images, differently from echocardiography, allow high quality tracking of the myocardial wall, which is an essential requirement for a reliable FT analysis (33).

### Study limitations

This is a retrospective, cross-sectional single centre study. Serial studies would be needed to explore whether alterations in strain values may timely precede changes in RV systolic function and confirm our hypothesis that CMR-FT could detect early signs of RV impairment in EA. The cohort of patients is of limited number, but this is due to the low incidence of EA. Population study concerns various age groups, including children. However, we did not include neonates or infants, in whom prognosis seems to be worst. Since patients were selected from clinical control studies, they belonged mostly to a good functional class.

### Conclusions

The functional RV in patients with EA is characterized by prevalent deterioration of the short-axis function with a significant reduction of global circumferential and radial strain. The transverse component of myocardial contraction seems to be predominantly impaired in EA, even in patients with an apparently preserved RV function as assessed by routine CMR parameters. CMR-FT is an advanced imaging tool that provides quantitative deformation values, which may detect subtle alterations of myocardial contraction with potential value in the clinical management of EA patients.

## Footnote

# References

1. Fratz S, Chung T, Greil GF, et al. Guidelines and protocols for cardiovascular magnetic resonance in children and adults with congenital heart disease: SCMR expert consensus group on congenital heart disease. J Cardiovasc Magn Reson 2013;15:51.

2. Mrad Agua K, Burri M, Cleuziou J, et al. Preoperative predictability of right ventricular failure following surgery for Ebstein's anomaly. Eur J Cardiothorac Surg 2019;55:1187-93.

3. Schuster A, Hor KN, Kowallick JT, et al. Cardiovascular Magnetic Resonance Myocardial Feature Tracking: Concepts and Clinical Applications. Circ Cardiovasc Imaging 2016;9:e004077.

4. Shehata ML, Cheng S, Osman NF, et al. Myocardial tissue tagging with cardiovascular magnetic resonance. J Cardiovasc Magn Reson 2009;11:55.

5. Guaricci AI, Masci PG, Muscogiuri G, et al. CarDiac magnEtic Resonance for prophylactic Implantable-cardioVerter defibrillAtor ThErapy in Non-Ischaemic dilated CardioMyopathy: an international Registry. Europace 2021;23:1072-83.

6. Chamsi-Pasha MA, Zhan Y, Debs D, et al. CMR in the Evaluation of Diastolic Dysfunction and Phenotyping of HFpEF: Current Role and Future Perspectives. JACC Cardiovasc Imaging 2020;13:283-96.

7. te Riele AS, Tandri H, Bluemke DA. Arrhythmogenic right ventricular cardiomyopathy (ARVC): cardiovascular magnetic resonance update. J Cardiovasc Magn Reson 2014;16:50.

8. Prihadi EA, van der Bijl P, Dietz M, et al. Prognostic Implications of Right Ventricular Free Wall Longitudinal Strain in Patients With Significant Functional Tricuspid Regurgitation. Circ Cardiovasc Imaging 2019;12:e008666.

9. Müller J, Kühn A, Tropschuh A, et al. Exercise performance in Ebstein's anomaly in the course of time - Deterioration in native patients and preserved function after tricuspid

10. Kühn A, De Pasquale Meyer G, Müller J, et al. Tricuspid valve surgery improves cardiac output and exercise performance in patients with Ebstein's anomaly. Int J Cardiol 2013;166:494-8.

11. EDWARDS JE. Pathologic features of ebstein's malformation of the tricuspid valve. Proc Staff Meet Mayo Clin 1952;28:89-94.

12. Paranon S, Acar P. Ebstein's anomaly of the tricuspid valve: from fetus to adult: congenital heart disease. Heart 2008;94:237-43.

13. Burri M, Mrad Agua K, Cleuziou J, et al. Cone versus conventional repair for Ebstein's anomaly. J Thorac Cardiovasc Surg 2020;160:1545-53.

14. Meierhofer C, Kühn A, Müller J, et al. Non-invasive Hemodynamic CMR Parameters Predicting Maximal Exercise Capacity in 54 Patients with Ebstein's Anomaly. Pediatr Cardiol 2019;40:792-8.

15. Fratz S, Schuhbaeck A, Buchner C, et al. Comparison of accuracy of axial slices versus short-axis slices for measuring ventricular volumes by cardiac magnetic resonance in patients with corrected tetralogy of fallot. Am J Cardiol 2009;103:1764-9.

16. Qureshi MY, Sommer RJ, Cabalka AK. Tricuspid Valve Imaging and Intervention in Pediatric and Adult Patients With Congenital Heart Disease. JACC Cardiovasc Imaging 2019;12:637-51.

17. Fratz S, Janello C, Müller D, et al. The functional right ventricle and tricuspid regurgitation in Ebstein's anomaly. Int J Cardiol 2013;167:258-61.

18. Fratz S, Hess J, Schuhbaeck A, et al. Routine clinical cardiovascular magnetic resonance in paediatric and adult congenital heart disease: patients, protocols, questions asked and contributions made. J Cardiovasc Magn Reson 2008;10:46.

19. Anderson KR, Lie JT. The right ventricular myocardium in Ebstein's anomaly: a morphometric histopathologic study. Mayo Clin Proc 1979;54:181-4.

20. Kempny A, Fernández-Jiménez R, Orwat S, et al. Quantification of biventricular myocardial function using cardiac magnetic resonance feature tracking, endocardial border delineation and echocardiographic speckle tracking in patients with repaired tetralogy of Fallot and healthy controls. J Cardiovasc Magn Reson 2012;14:32.

21. Lee CM, Sheehan FH, Bouzas B, et al. The shape and function of the right ventricle in Ebstein's anomaly. Int J Cardiol 2013;167:704-10.

22. Anderson KR, Lie JT. Pathologic anatomy of Ebstein's

anomaly of the heart revisited. Am J Cardiol 1978;41:739-45.

23. Anderson KR, Zuberbuhler JR, Anderson RH, et al. Morphologic spectrum of Ebstein's anomaly of the heart: a review. Mayo Clin Proc 1979;54:174-80.

24. Sanchez-Quintana D, Anderson RH, Ho SY. Ventricular myoarchitecture in tetralogy of Fallot. Heart 1996;76:280-6.

25. Pettersen E, Helle-Valle T, Edvardsen T, et al. Contraction pattern of the systemic right ventricle shift from longitudinal to circumferential shortening and absent global ventricular torsion. J Am Coll Cardiol 2007;49:2450-6.

26. Guglielmo M, Fusini L, Muscogiuri G, et al. T1 mapping and cardiac magnetic resonance feature tracking in mitral valve prolapse. Eur Radiol 2021;31:1100-9.

27. Kühn A, Meierhofer C, Rutz T, et al. Non-volumetric echocardiographic indices and qualitative assessment of right ventricular systolic function in Ebstein's anomaly: comparison with CMR-derived ejection fraction in 49 patients. Eur Heart J Cardiovasc Imaging 2016;17:930-5.

28. Steinmetz M, Broder M, Hösch O, et al. Atrio-ventricular deformation and heart failure in Ebstein's Anomaly - A cardiovascular magnetic resonance study. Int J Cardiol 2018;257:54-61.

29. Valsangiacomo Buechel ER, Mertens LL. Imaging the right heart: the use of integrated multimodality imaging. Eur Heart J 2012;33:949-60.

30. Steinmetz M, Usenbenz S, Kowallick JT, et al. Left ventricular synchrony, torsion, and recoil mechanics in Ebstein's anomaly: insights from cardiovascular magnetic resonance. J Cardiovasc Magn Reson 2017;19:101.

31. Yang D, Li X, Sun JY, et al. Cardiovascular magnetic resonance evidence of myocardial fibrosis and its clinical significance in adolescent and adult patients with Ebstein's anomaly. J Cardiovasc Magn Reson 2018;20:69.

32. Prota C, Di Salvo G, Sabatino J, et al. Prognostic value of echocardiographic parameters in pediatric patients with Ebstein's anomaly. Int J Cardiol 2019;278:76-83.

33. Truong VT, Safdar KS, Kalra DK, et al. Cardiac magnetic resonance tissue tracking in right ventricle: Feasibility and normal values. Magn Reson Imaging 2017;38:189-95.